J. Membrane Biol. 111, 215–227 (1989)

The Journal of
Membrane Biology

Membrane and Junctional Properties of Dissociated Frog Lens Epithelial Cells

Kim Cooper, James L. Rae, and Peter Gates
Department of Physiology and Biophysics, and Department of Ophthalmology, Mayo Foundation, Rochester, Minnesota 55905

Summary. Individual cells and cell pairs were isolated from frog lens epithelium. Individual cells were whole cell voltage clamped and the current-voltage relationship was determined. The cells had a mean resting voltage of −54.3 mV and a mean input resistance of 1.4 GΩ. The current-voltage relationship was linear near the cell resting voltage, but showed decreased resistance with large depolarization or hyperpolarization. Junctional currents between pairs of cells were recorded using the dual whole cell voltage-clamp technique. The corrected junctional resistance was 15.5 MΩ (64.5 nS). The junctional current-voltage relationship was linear. A combination of ATP and cAMP, in the electodes, stabilized junctional resistance. Currents recorded when uncoupling was nearly complete, showed evidence of single connexon gating events. A single-channel conductance of about 100 pS was prominent. Dye spread between isolated cell pairs was demonstrated using Lucifer Yellow CH in a whole cell configuration. Photodamage to the cells due to the dye was apparent. Dye loaded cells, in the presence of exciting light, showed decreased resting voltages, decreased input resistances and morphological changes. Glutathione (20 mM) delayed this damage.

Key Words lens · epithelium · gap junctions · membrane transport · whole cell voltage clamp · dye transfer

Introduction

The role of the lens in vision is to act as a focusing element that allows the organism to see both near and distant objects. The mechanism for this accommodation varies enormously from species to species (Sivac, 1980). Regardless of the mechanism of accommodation, lens function requires transparency and a high refractive index. Transparency is accomplished by producing a large mass of specialized cells, the fiber cells, which lack most organelles and are packed in an orderly array with very little extracellular space (1–5% volume fraction). The fiber cells also have a very high protein content (35 g/100 ml compared to 20 g/100 ml in muscle), which gives rise to the lens' high refractive index (average value 1.420). Short range interactions between the proteins reduce the light scattering that would otherwise result if the proteins behaved as independent scatterers (Bettelheim, 1985). One consequence of these properties is that the fiber cells themselves are incapable of much metabolic activity. Thus, the lens epithelium must act as the primary transporter of many substances for the entire lens mass.

One mechanism that could assist the epithelium with this transport load is the hypothetical lens internal circulation (Mathias, 1985). According to this hypothesis, fluid flows in the extracellular space from surface to center, crosses the cell membranes and then flows back to the surface inside the cells. This system requires that the lens cells be extensively internally coupled. A spatial segregation of different conductances sets up standing current loops. Fluid movement follows this ionic movement, thus the surface cells must have different membrane conductance properties than the nonsurface cells. Detailed information about the membrane and junctional properties of cells from different parts of the lens is essential to test this hypothesis.

Cell-to-cell communication in the lens has been demonstrated using electrical recording, dye transfer and other techniques (reviewed in Mathias & Rae, 1989). Dye injected into a fiber cell enters adjacent fiber cells. In isolated epithelial sheets, dye injected at one point spreads to other neighboring epithelial cells (Duncan et al., 1988; Stewart et al., 1988). In one case, it has been shown that dye injected into fiber cells will eventually spread to the connected epithelial cells (Miller & Goodenough, 1986). Thus, it appears as if all cell types in the lens intercommunicate via gap junctions. Coupling between lens cells can also be demonstrated by injecting current with one electrode and following its spread with a second electrode. The dye and current spread is assumed to occur via gap junctions similar to those found in other tissues. Biochemical and morphological studies show that the lens contains some junctions that are not identical to

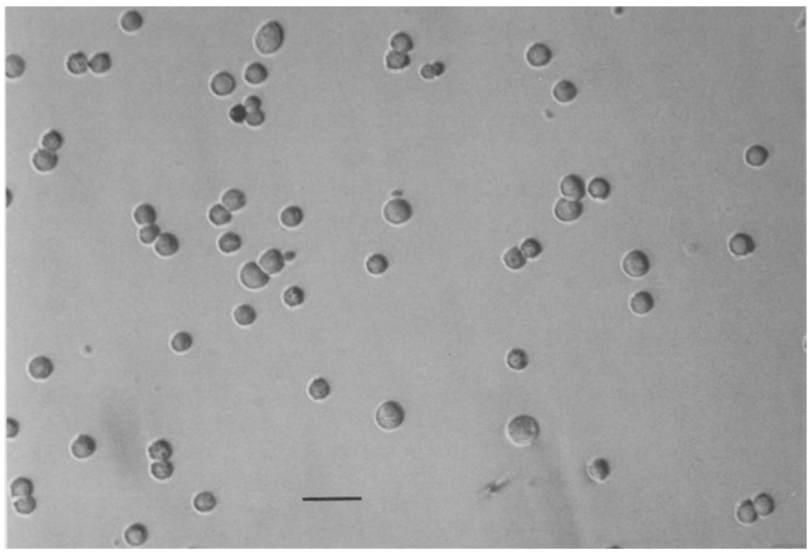

Fig. 1. Morphology of dissociated frog lens epithelial cells. Scale bar 40 μm

those in other tissues (Nicholson et al., 1983; Revel et al., 1986; Beyer, Goodenough & Paul, 1988). To add to the complexity, it is becoming apparent that several types of junctions exist in the lens (reviewed in Mathias & Rae, 1989). Junctions between epithelial cells are different from those between fiber cells. Also the properties of fiber cell junctions in the cortex may differ from those in the nucleus. Functional measurements on fiber cell junctions seem to indicate that they are controlled by H^+, Ca^{2+}, cAMP or calmodulin as are many other junctions (Campos de Carvalho, 1988; Peracchia, 1988). Direct measurement of junctional currents in isolated cell pairs from different parts of the lens will help unravel the complexities of junctional communication in this tissue.

Much of the existing data on regional variation of lens membrane conductance is based on indirect inference from impedance and ion substitution experiments. These studies indicate that the surface cells have most of the lens' K^+ conductance and that the deeper cells contain most of the Na^+ and Cl^- conductance (Mathias et al., 1985). Detailed measurements of conductance mechanisms in isolated sheets of lens epithelium have been made using the patch-clamp technique (Rae, 1984, 1985; Rae & Levis, 1984; Jacob, 1984, 1988; Jacob, Bangham & Duncan, 1985; Rae, Levis & Eisenberg, 1988), and have shown wide variation in channel types from one species to another. Characterization of membrane resistance in an epithelial sheet using measurements of input resistance are notoriously inacurrate (Jack, Noble & Tsien, 1975 (p. 91)). In this paper, we present results obtained using a combination of the whole cell voltage-clamp technique (Marty & Neher, 1983) and cell dissociation. We have measured the properties of junctions and membrane conductances from frog lens epithelial cells. We report membrane and junctional current-voltage relationships. The junctional resistance stability was found to be dependent on the existence of ATP and cAMP in the pipette perfusion solution. We also report the measurement of current through single gap junction molecules. The current-voltage relationship at the single-channel level gave a conductance of 118 pS.

Materials and Methods

Cell Dissociation

Rana pipiens were stored at room temperature and fed daily. The eyes were removed and the lenses dissected free from the globe using standard techniques. The lens capsule was peeled from the posterior surface and pinned to a Sylgard disc. The fiber cell mass was then removed and the remaining epithelial sheet—capsule preparation was cleaned of any adhering fiber cell debris (Rae, 1985). The disc holding the epithelium was transferred to a petri dish containing normal frog Ringer to which had been added 0.1% trypsin (Sigma type III) and 2 mM EGTA. The cells remained in this solution for 10–30 min. At the end of this period, the disc was placed in a 15-ml conical tube containing 5 ml of normal Ringer. The cells were triturated with a Pasteur pipette for approximately 1 min. This removed the cells from the capsule and left them suspended in solution. The solution was then transferred to a 35-mm tissue culture dish and the cells were allowed to settle for 10 min. Most cells attached to the dish within this time. The cells could be maintained in a healthy state for some time, especially if antibiotic (penicillin 10,000 U plus streptomycin 10 mg) was added to 100 ml of Ringer solution.

Figure 1 shows the kinds of cells found in such a preparation. Most cells were completely separated from their neighbors

and were roughly spherical with a mean diameter of about 17 μm. In healthy cells, the nucleus was not visible with Schlieren microscopy and the cell surface was neither perfectly smooth nor heavily pitted. In any isolation, some of the cells did not completely dissociate and thus cell pairs, triplets, etc., were present. Cells with lengths up to a few hundred μm were also seen. These may have been elongating cells from the equatorial region or perhaps resealed fragments of fiber cells missed in the cleaning procedure.

Whole Cell Recording

The 35-mm tissue culture dish used in the dissociation fit into a custom-built stage attached to a stand, which allowed viewing of the preparation with a Nikon Diaphot fluorescence inverted microscope. The stand also supported a pair of micromanipulator systems (Klinger Scientific, Richmond NY) which held the head stages of two patch clamps (model 1-B, Axon Instruments, Burlingame, CA). This arrangement allowed recording of single-channel or whole cell currents from the isolated cells (Rae & Levis, 1984; Rae et al., 1988). Data were digitized using a 12-bit A/D converter with a maximum digitization rate of 30 kHz (model TL-1, Axon Instruments). Data were taken through an antialiasing filter (4-pole Bessel) into either an IBM-AT computer or a RACAL Store4DS tape recorder, and later analyzed using a commercial software package (PCLAMP, Axon Instruments). All experiments were done at room temperature.

We tested for the possibility that leachable components from the glass might affect the whole cell currents (Cota & Armstrong, 1988; Furman & Tanaka, 1988; Rae et al., 1988; Rojas & Zuazaga, 1988) by making electrodes from three different glasses; 7052 (a low-lead glass, <0.003 M), 8161 and KG-12 (both high lead glasses, 9.2 and 4 M, respectively). All electrodes used had resistances in the range 5–15 MΩ.

Junctional Current Recording

Independent recording from both cells of an isolated pair was achieved using the two patch-clamp systems (Neyton & Trautmann, 1985; White et al., 1985; Veenstra & DeHaan, 1986; Weingart, 1986; Somogyi & Kolb, 1988). This approach allowed measurement of either the membrane properties of the individual cells or the properties of the junctional region between the cells. By measuring junctional currents well into the period of uncoupling, single-channel currents from gap junction molecules could be recorded. In order to maximize the signal-to-noise ratio when recording single gap junction events, we decreased the membrane noise by replacing the bath solution with impermeant ions (N-methyl-D-glucamine-methane-sulphonic acid) and used a membrane impermeant anion (methane-sulphonic acid) in the pipette solutions.

Dye Coupling Measurements

Dye transfer between cells in isolated groups was demonstrated by placing fluorescent dye in the internal solution of one whole cell electrode. We used 5 mM concentrations of either Lucifer Yellow CH or carboxyfluorescein for these experiments. The dyes were excited with light from a mercury vapor lamp (HBO 100 W) using the following Nikon filters: excitation filter (EX435), barrier filter (BA520), and dichroic mirror (DM510).

Table 1.

Soln.	X	Na_2ATP	$CaCl_2$[a]	K_2EGTA
1	Asp	0	0	1
2	Asp	5	0	1
3	Asp	5	0	0
4	Asp	5	1	3
5	Cl	5	0	0
6	Cl	5	1	3

All entries are in mM. Asp = aspartate.
[a] No $CaCl_2$ was added to the solution. Contaminant Ca was assumed to be 10 μM.

Solutions

The composition of the normal Ringer's solution was (in mM): Na 104.5, K 2.5, Cl 114, Ca 2.0, Mg 1.5, HEPES 5.0, glucose 5.0, with pH 7.35 and osmolality 210 mOsm/kg. The internal solutions used for whole cell recordings are shown in Table 1. All internal solutions had NaCl 5.0, $MgCl_2$ 1.5, HEPES 5.0, KX 91.0 (where X is the anion stated), osmolality 214 mOsm/kg and pH 7.00.

Results

Whole Cell Recording

Resting Voltage

We report resting voltages from 100 isolated frog lens epithelial cells. Pipette offsets were adjusted to zero in the bath before touching the electrode to the cell. A seal was then formed, and a holding potential of −40 mV was applied to the pipette. The membrane in the patch was subsequently ruptured with a pulse of suction or voltage. Fewer seals were lost using suction than using voltage pulses. After a whole cell configuration was achieved, the membrane current was set to zero. The required voltage was taken to be the resting voltage of the cell.

Resting voltages were measured in all the solutions listed in Table 1. Table 2 shows the results of these measurements. The resting voltage did not depend significantly on whether the internal anion was Cl^- or aspartate, nor did it depend on the presence or absence of ATP. However, the resting voltage was somewhat depolarized in the high Ca^{2+} (10 μM) solution (statistically significant at the 2.5% level). Combining all the data from the low Ca^{2+} internal solutions, yielded a resting voltage of -54.3 ± 3.2 mV (mean ± SEM).

Table 2.

Soln.	Free Ca	V_{rest} (mV) ± SEM	R_{in} (GΩ) ± SEM	n	Comments
1	2 nM	−46.5 ± 7.7	1.17 ± 0.12	8	8161
2	2 nM	−51.7 ± 7.3	1.66 ± 0.27	12	8161
3	10 μM	−39.4 ± 1.1	1.38 ± 0.20	20	KG-12,8161
4	200 nM	−51.9 ± 11.3	1.58 ± 0.42	9	KG-12
5	10 μM	−45.0 ± 1.4	0.69 ± 0.17	14	KG-12
6a	200 nM	−57.4 ± 5.3	1.05 ± 0.15	20	KG-12,7052
6b	200 nM	−61.1 ± 1.8	2.05 ± 0.34	8	7052,CF
6c	200 nM	−54.2 ± 1.6	1.44 ± 0.33	9	7052,LY

Solutions 1–4 contained Asp as the anion, and solutions 5 and 6 contained Cl. All solutions contained ATP except solution 1. CF = carboxyfluorecein, LY = Lucifer Yellow CH. Solutions to which no Ca was added were assumed to contain 10 μM of contaminant Ca. 8161, 7052 and KG-12 are the glasses described in Materials and Methods.

Capacitance

Cell capacitance was also measured for many of the cells. The electrode capacitance was compensated after forming a giga-seal but before achieving the whole cell configuration. The membrane in the patch was then ruptured and the additional capacitance due to the cell was measured and compensated. We measured the cell diameter (D), assumed the cells to be spherical, and calculated the cell surface areas as πD^2. This was done on 45 cells with diameters ranging over an order of magnitude. Figure 2 shows how the measured cell capacitance varied with the calculated membrane area. The solid line is the result expected for a specific capacitance of 1 $\mu F/cm^2$.

It was a consistent observation that the whole cell capacitance decreased during the recording period. In one representative experiment, there was a 38% decrease in capacitance over a period of 30 min. This was accompanied by a 25% decrease in cell diameter and a change in cell morphology. The cells developed noticeable pits on their surfaces as the capacitance decreased.

Input Resistance

The input resistance was measured by applying a 10–20 mV square pulse to the pipette interior, in voltage-clamp mode, and recording the resulting current. This current contains contributions from both the membrane and the seal but is predominantly membrane current as long as the seal resistance is much larger than the cell input resistance. The ratio of the voltage-step amplitude to the steady-state current amplitude gave the input resistance, assuming a negligible voltage drop across the access resistance. For example, a membrane current of 100 pA flowing across a 30-MΩ access resistance would give rise to a 3-mV error.

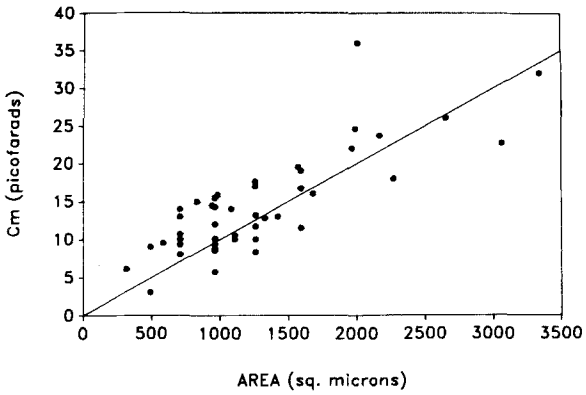

Fig. 2. Cell capacitance *versus* calculated cell area. The solid line represents 1 $\mu F/cm^2$

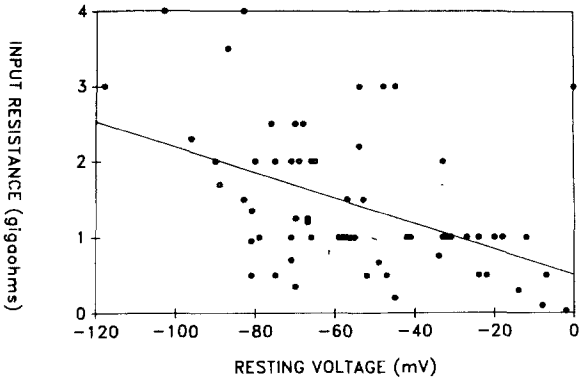

Fig. 3. Correlation between input resistance and resting voltage. The solid line is a linear regression. The correlation coefficient was 0.472

The input resistances were measured in all of the internal solutions listed in Table 1. Table 2 summarizes the data. As with the resting voltage, there was no statistically significant dependence on the particular internal anion used or on ATP level. Comparing all data with an internal Ca^{2+} of 10 μM with all data having an internal Ca^{2+} of 200 nM, showed no significant difference in input resistance. Combining all the data with low internal Ca^{2+} gave an input resistance of 1.42 ± 0.12 GΩ (mean ± SEM). The relationship between resting voltage and input resistance is shown in Fig. 3. There is a positive correlation (correlation coefficient 0.472) as shown by the solid line.

Current-Voltage Relationship

Current-voltage relationships (I-Vs) were obtained using the ramp-clamp technique. In this technique, a voltage range and a ramp duration were specified.

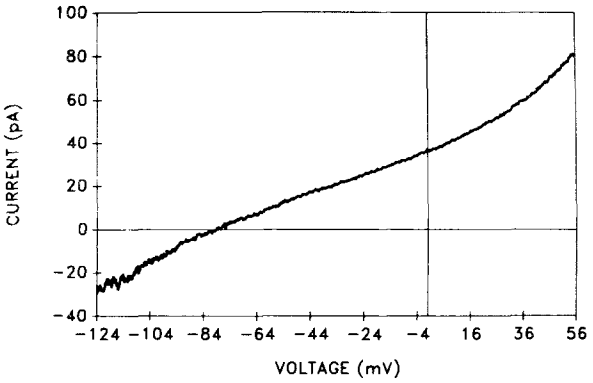

Fig. 4. Single-cell current-voltage relationship obtained by ramp voltage clamp. The duration of the ramp was 1 sec. The cell resting voltage was −79 mV, and the input resistance was 2.2 GΩ near the resting voltage. This *I-V* is the average of five runs. The electrode contained solution 3

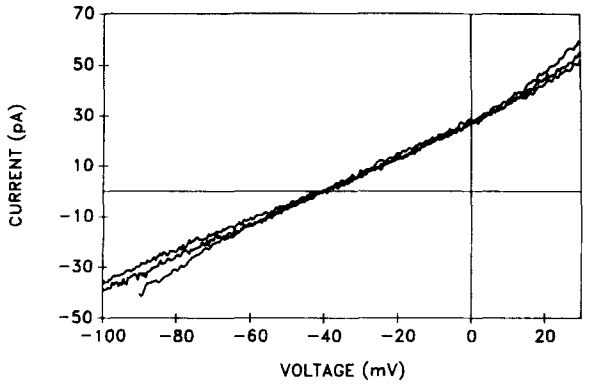

Fig. 5. Single-cell current-voltage relationships at three different ramp rates. Ramp durations were: 300 msec for the top trace, 3 sec for the middle trace and 30 msec for the bottom trace. The cells were held at −70 mV, the input resistance was 1.25 GΩ and the electrode contained solution 6

The computer then produced a series of equally spaced voltage steps (usually 1000) that spanned the desired voltage range. This effectively produced a ramp of voltage. An arbitrary number of *I-V*s could be averaged before storing the data. The resulting current was displayed as an *I-V* by relabeling the abscissa in terms of voltage instead of time. Figure 4 shows a typical result of such an experiment. In this case five *I-V*s were averaged together. The cell had a resting voltage of −79 mV and an input resistance of 2.2 GΩ. The *I-V* was fairly linear over the physiological range but showed a decrease in resistance at large positive or negative voltages. We tested for voltage-dependent gating phenomena by applying ramps of varying duration. A ramp whose rate is rapid relative to the rate of any voltage-dependent gating process would measure the desired instantaneous *I-V*. A ramp applied more slowly would allow time for the channels to change their open probability, in response to voltage, and the current would reflect this change. Such voltage dependence would appear as a change in the shape of the *I-V* with different ramp speeds. An example of such an experiment is shown in Fig. 5, there was no convincing voltage dependence. This was true of most cells. Occasionally evidence of voltage dependence was noted. As seen in Fig. 6*A*, step protocols revealed a current that resembled the classical delayed rectifier. Like the delayed rectifier the current was blocked by Ba^{2+} (Fig. 6*B*).

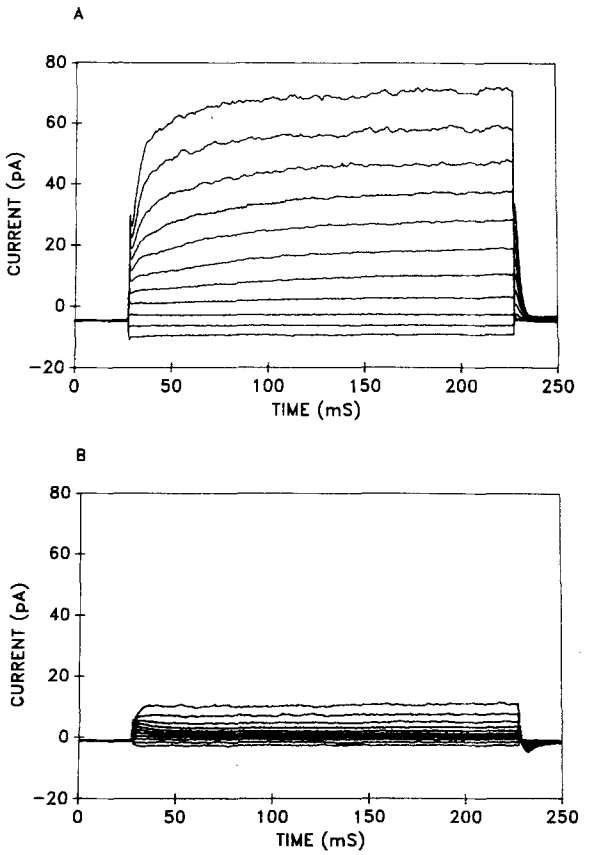

Fig. 6. Time-dependent membrane current. (*A*) In control solution. (*B*) In the presence of 5 mM Ba^{2+}

Electrode Glasses

Recent reports have shown that currents recorded with the whole cell technique can be affected by the specific glass used (Cota & Armstrong, 1988; Furman & Tanaka, 1988; Rojas & Zuazaga, 1988). It appears that high-lead glasses are more likely to cause problems. EGTA buffering has been shown to be effective at reducing the effects of the high-lead glasses. We measured resting voltages and input resistances using various combinations of electrode

Table 3.

Glass	EGTA (mM)	V_{rest} (mV) ± SEM	R_{in} (GΩ)	n
7052	3	−59.2 ± 4.7	1.50 ± 0.18	25
KG-12	0	−43.8 ± 4.8	0.97 ± 0.12	29
KG-12	3	−52.9 ± 6.5	1.29 ± 0.23	21
8161	0	−23.0 ± 5.6	1.76 ± 0.28	0
8161	3	−50.5 ± 5.6	1.49 ± 0.19	19

glass and EGTA buffering. This data is presented in Table 3. The only statistically significant effect was that of 8161 (the highest lead glass) on the resting voltage in the absence of EGTA (significant at the 0.5% level). No changes were seen in the shape of the *I-V*s with different glasses or EGTA buffering levels.

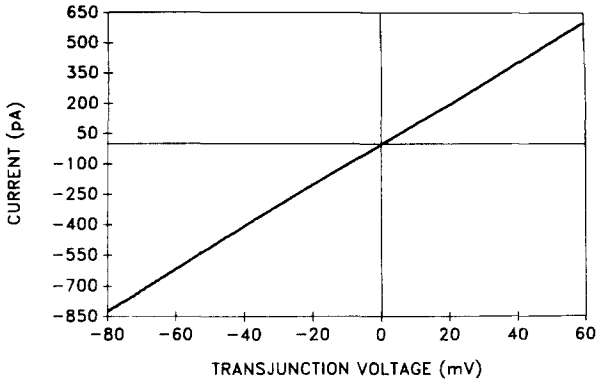

Fig. 7. Junctional membrane current-voltage relationship from a ramp voltage clamp. The total time for the ramp was 100 msec. The junctional resistance was 98.3 MΩ. The electrode contained solution 5. The cells' resting voltages were −47 mV and their input resistances were 500 and 200 MΩ. This *I-V* is the average of five runs

Junctional Recording

Current-Voltage Relationship

We recorded junctional currents from 40 cell pairs using the double whole cell technique. After achieving whole cell configurations on both cells of a pair, the electrode currents were both set to zero. This usually resulted in the two cells being held at nearly the same voltage. If the electrode voltages were the same, and the access resistances of the two electrodes were the same, no current would flow across the junction in the resting situation. A step or ramp in voltage applied to both cells simultaneously would cause no current to flow across the junction, and thus would allow the recording of membrane current from both cells at once. However, when the step or ramp was applied to only one cell of the pair, the current produced by the voltage clamp in the cell would be the sum of currents flowing across the surface membrane and the junction. When the first cell is stepped to its new voltage, current from the second cell begins to flow across the junction. To prevent this from changing the voltage in the second cell, its voltage-clamp circuitry must supply a current equal and opposite to that flowing across the junction. This can be measured as the junctional current (Spray, Harris & Bennett, 1981).

Junctional *I-V*s were obtained using the ramp voltage-clamp version of the above technique. Figure 7 shows a representative *I-V* produced by applying a voltage ramp of 1000 steps between +60 mV and −80 mV relative to rest. This curve was the average of five *I-V*s. Note that the junctional current was a linear function of transjunctional voltage. The zero current point was within a few millivolts of zero voltage. This is to be expected, since the internal solutions in the two cells were identical. The junctional resistance of the cell pair shown in Fig. 7 was 98.3 MΩ. The junctional resistances measured in the 40 cells ranged from 15.7 to 607 MΩ. Figure 8*A* shows the distribution of these resistances. There is clear evidence of two populations. The four measured resistances with values above 500 MΩ represent a small population of relatively poorly coupled cell pairs. Figure 8*B* shows the distribution of the remaining 36 cell pairs. The mean resistance of all 40 pairs was 123.7 ± 1.9 (SEM) MΩ. Excluding the four large resistance pairs, the mean was 79.0 ± 1.3 (SEM) MΩ. These values were not corrected for access resistance (Neyton & Trautmann, 1985; Weingart, 1986). When the access resistance of the recording electrodes becomes comparable to the junctional resistance, some of the applied voltage drops across the access resistances. This causes an overestimate of the driving force for current flow across the junction and hence an overestimate of the junctional resistance. The correction for access resistance is given by the following formula

$$R_j = R_{jm} - R_{a1} - R_{a2} \quad (1)$$

where R_j is the actual junctional resistance, R_{jm} is the measured junctional resistance, and R_{a1} and R_{a2} are the access resistances of the two electrodes. The corrections could be substantial. For example, the corrected junctional resistance of the record shown in Fig. 7 was 70 MΩ. The mean access resistance from 61 measurements was 31.8 ± 0.6 (SEM)

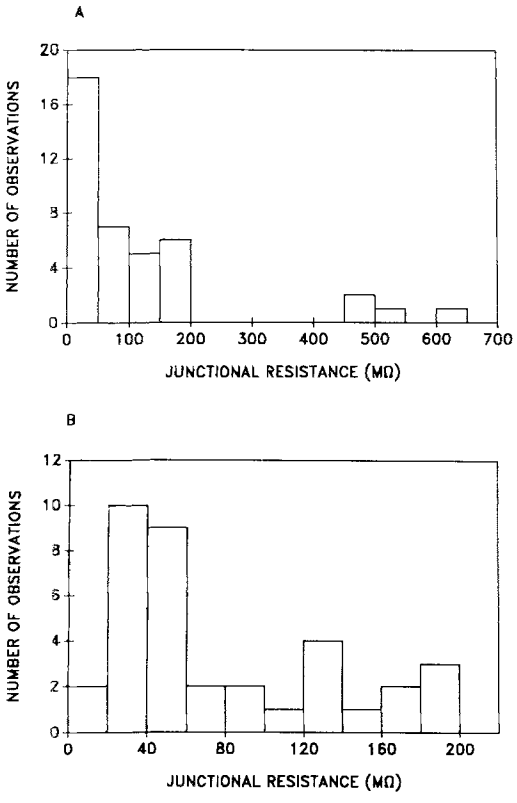

Fig. 8. Histograms of junctional resistance. (*A*) Histogram of all 40 cell pairs studied. Data not corrected for access resistance effects. (*B*) Histogram of the 36 cell pairs in the low resistance group

MΩ. Applying this to the 36 measurements reported above yields an estimate of junctional resistance of 15.5 MΩ. The *I-V*'s were linear for all of the cell pairs studied regardless of the value of the junctional resistance. No time dependence of the junctional current was seen over a time scale from 50 msec to 1 sec (Fig. 9).

The junctional resistance, in any given cell pair, was found to increase with time until the cells became completely uncoupled. Similar uncoupling has been seen in many other preparations using this technique. Recently Somogyi and Kolb (1988) demonstrated that a mixture of ATP and cAMP would extend the lifetime of coupling in pancreatic acinar cells. We tested this in our preparation by examining the stability of coupling in eight cell pairs. Four of the pairs were patch clamped with no ATP or cAMP in the pipette. The mean time to 50% uncoupling was 30.25 min (Fig. 10*A*). In four other cell pairs, the pipettes contained 5.4 mM ATP and 1 mM cAMP (Fig. 10*B*). Two of these cell pairs remained coupled for 60 min, while the other two were still coupled at the termination of recording at about 120 min.

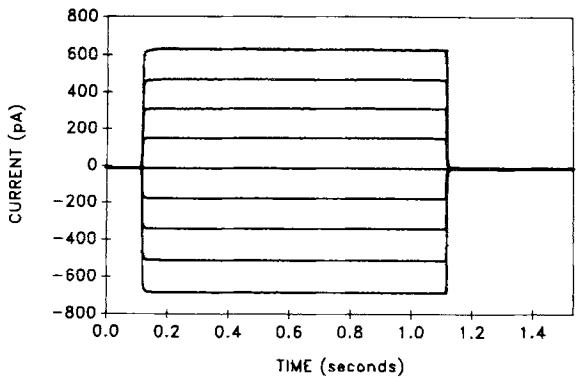

Fig. 9. Junctional current in response to voltage steps. This is the average of five runs. The steps were made from the resting voltage of −47 mV. The most hyperpolarized step was to −127 mV. Eight subsequent steps were made in increments of 20 mV. The junctional resistance was 122 MΩ. The electrode contained solution 6. The step duration was 1 sec

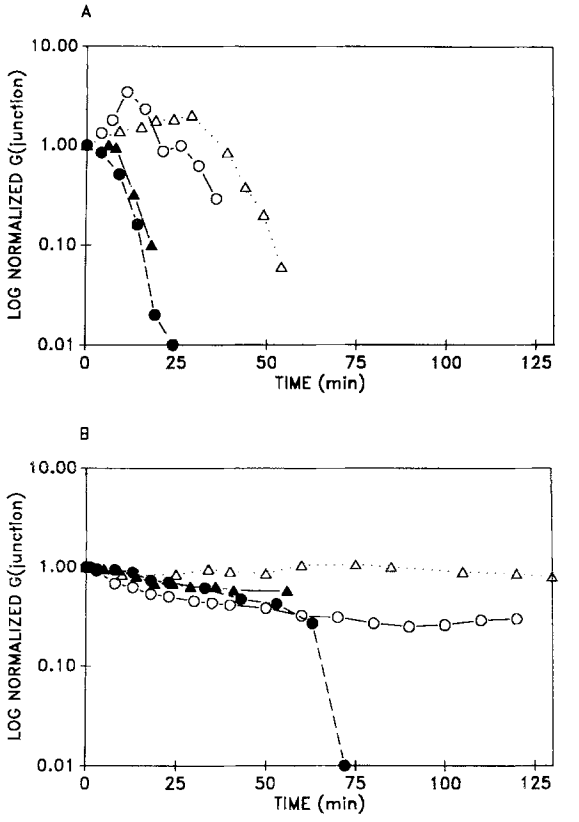

Fig. 10. (*A*) Normalized junctional conductance as a function of time with 0 ATP and 0 cAMP in the pipettes. (*B*) Same protocol but with 5.4 mM ATP and 1 mM cAMP in the pipettes

As the cell pairs uncoupled, a point was reached at which only a small number of channels were still gating in the junction. High resolution recordings at this time allowed the visualization of individual gap junction channel-gating transitions

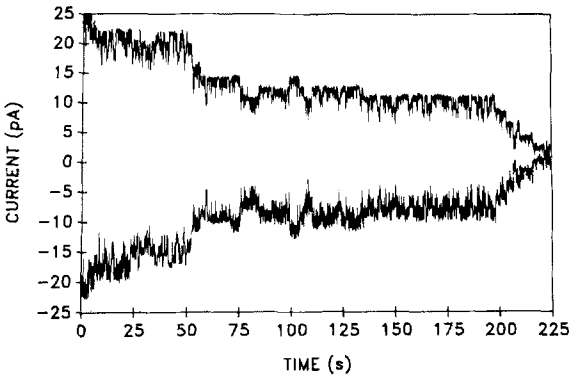

Fig. 11. High resolution recordings of junctional current well into the uncoupling period. Top and bottom traces are simultaneous recordings from both patch clamps. There was a 20-mV driving force across the junction. The data was filtered at 10 Hz and sampled at 20 Hz

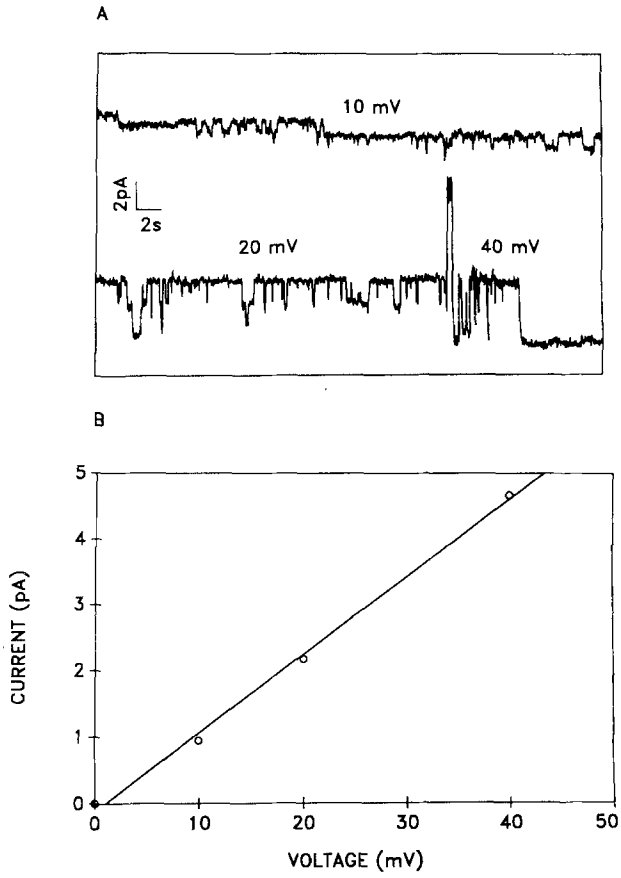

Fig. 12. (*A*) Single gap junction channel events at several voltages. Data filtered at 40 Hz and digitized at 200 Hz. (*B*) Current-voltage relationship of junctional channel. Single-channel conductance 118 pS

(Fig. 11). Opening and closing of junctional channels can be distinguished from opening and closing of surface membrane channels in two ways. First, when a channel opens in the junction, the currents flowing in the two patch clamps will be of opposite polarity. The response to the opening of a surface membrane channel is of the same polarity in the two patch clamps. Second, the amplitude of a junction event is expected to be of roughly the same amplitude in the two recordings while the response to a surface channel opening is much larger in the patch clamp connected to the cell in which the opening occurs. In the other clamp, the current is attenuated because it must traverse the junction, which is now of high resistance because of the uncoupling.

In another experiment, several voltages were applied across the junction during uncoupling. This allowed the measurement of a junctional *I-V* (Fig. 12). The *I-V* was linear and the conductance was 118 pS. Individual openings were seconds in duration.

Dye Coupling

We were able to observe dye coupling between cells of isolated pairs using Lucifer Yellow CH (Fig. 13). Complete dye equilibration between the cells was only observed when the exciting light source was left off for a few minutes after the whole cell configuration was achieved. Illumination of a dye-loaded cell caused a decrease in cell input resistance that progressed with time after exposure to the exciting light. Figure 14 shows the current response, to repeated 10-mV depolarizing pulses, of a cell containing Lucifer Yellow CH, in the presence of exciting light. The amplitude of this current is a measure of input resistance. Over a period of 60 sec, the input resistance dropped from a value of 500 MΩ, before the exciting light was turned on, to a value of 30 MΩ. The resting voltage decreased to 0 mV during this same time. This fall in resting voltage is reflected in the shifting baseline in Fig. 14. The effects were not reversible. Such damage was not observed in dye-loaded cells in the absence of exciting light, as can be seen in the last two rows of Table 2. Also cells exposed to exciting light in the absence of dye showed no signs of damage. Similar dye damage was seen with carboxyfluorescein. Further evidence of damage is apparent in Fig. 15. Both the dye-injected cell and the cell to which it was coupled developed large surface membrane protrusions. Dye-damaged cells often developed such surface protrusions and eventually ruptured.

In an attempt to reduce the photodamage, we included 20 mM glutathione in the pipette. As shown in Fig. 16, this slowed the rate of damage but did not eliminate it. Similar results were obtained

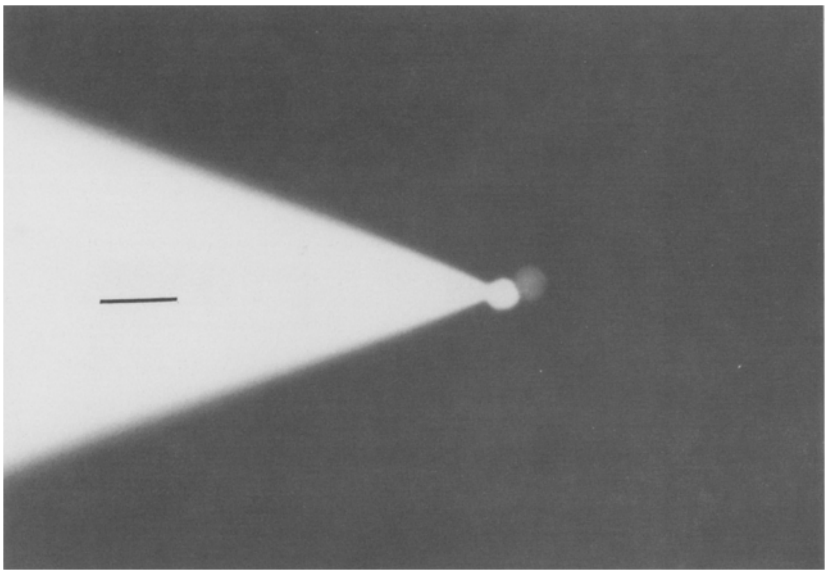

Fig. 13. Lucifer Yellow CH spread in a cell pair. Scale bar 40 μm

with 20 mM ascorbate. Dithiothreotol (DTT), at 1 mM, had no noticeable effect on the photodamage. The damage could be reduced using neutral density filters (2 log unit or greater), but with enough filtering to make the damage minimal we could not visualize the cells adequately.

Discussion

We have shown the feasibility of recording whole cell and junctional currents from isolated lens epithelial cells. We need to demonstrate the extent to which these cells have been altered in the isolation procedure. One way to assess this is to compare the properties of the isolated cells with properties deduced from experiments on whole lens and isolated epithelial sheets.

The cells had a mean resting voltage of -54.3 ± 3.2 mV. Intact frog lenses have a mean resting voltage of -75.2 ± 1.1 mV (Rae & Germer, 1974). The measurements of resting voltages in isolated frog lens epithelial sheets are somewhat variable. The reported values are -54.6 ± 1.1 mV (Jacob, 1984), -56.1 ± 2.3 mV (Cooper et al., 1986) and -79.0 ± 0.9 mV (Duncan et al., 1988). Thus, our cells have somewhat depolarized resting voltages on average. We assume that the healthier cells had the more negative resting voltages and that the less healthy cells had the more positive values. The less healthy cells may have been damaged as a result of the dissociation procedure, even though our methods are less harsh than those used for many other tissues.

The cells had a mean input resistance of 1.4 ± 0.12 GΩ. The input resistances from single dissociated cells can be compared with input resistances of whole lens and isolated epithelial sheets by expressing all three as area-specific resistances. The results in Fig. 2 imply that an estimate of cell area based on measured cell diameter is acceptable. Given an average cell diameter of 17 μm, and assuming a spherical cell, our measurements yield an area-specific resistance of 12.6 kΩcm^2. This number is about twice as large as the estimate of area-specific resistance reported by Mathias, Rae and Eisenberg (1979) for whole frog lenses (surface cells only). It is about half as large as that reported by Duncan et al. (1988) for isolated frog lens epithelial sheets. Given

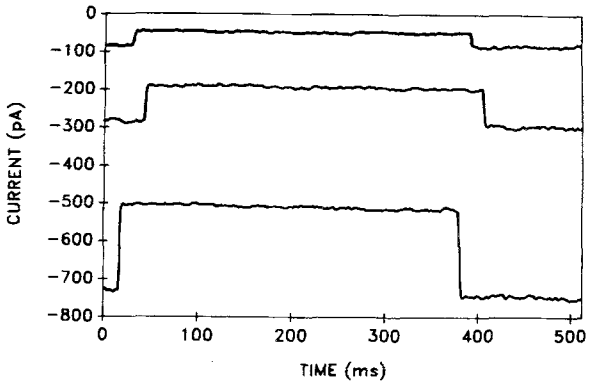

Fig. 14. Cell current response to repetitive 10-mV steps in a Lucifer Yellow CH filled cell after illumination with exciting light. The pulses were delivered once every second and had a pulse duration of 350 msec. The electrode contained solution 6, with 5 mM Lucifer Yellow CH. The top trace is the second pulse, the middle trace is the 25th pulse and the bottom trace is the 50th pulse. The cell was held at a constant holding potential of -35 mV

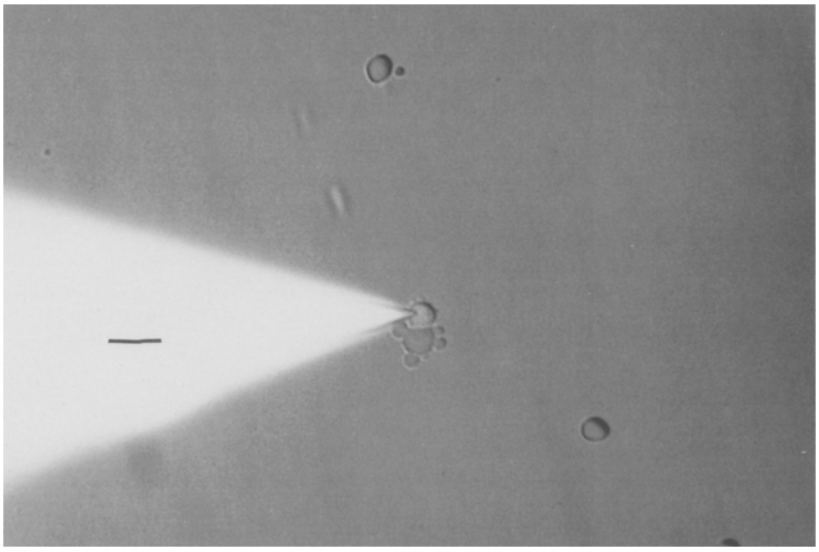

Fig. 15. Cell damage as a result of fluorescent illumination in the presence of Lucifer Yellow CH in the pipette. Scale bar 40 μm

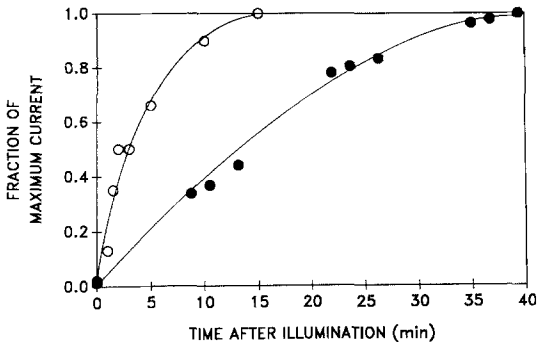

Fig. 16. Fraction of maximum current after illumination in Lucifer Yellow CH containing cells. The open circles are with pipette solution 6 with 5 mM Lucifer Yellow CH. The filled circles have the same solution but with 20 mM glutathione

the uncertainties in all three techniques, the numbers from the different preparations are in reasonable agreement. The input resistances were not significantly different with aspartate *versus* Cl^- as internal anion, with or without ATP, or with 10 μM *versus* 200 nM internal Ca^{2+}. The shape of the whole cell current-voltage relationship is linear around the resting voltage with an increase in current at large positive and negative voltages. This is in agreement with earlier work done on these cells by Rae (1985).

The channel basis for the *I-V* is uncertain. Numerous on-cell patch-clamp recordings from frog lens epithelial cells by different investigators (Rae & Levis, 1984; Jacob et al., 1985; Rae, 1985; Cooper et al., 1986) have failed to find a significant density of K^+ channels. The occasional appearance of the delayed rectifier K^+ conductance in these cells is suggestive that they may play a part in determining the normal resisting voltage. Specific experiments to test this possibility should be performed.

In order to compare the measured junctional resistance with that obtained in epithelial sheets, we modeled an epithelial sheet as a plate of close packed hexagonal cells. By comparing the differential resistance of a ring of cells with that of a ring of the homogeneous medium, we derived the result that the resistance between two isolated cells should be

$$R_j = 9\, R_i/(\pi\, b) \qquad (2)$$

where R_j is the resistance between two isolated cells, R_i is the specific resistivity of the homogeneous sheet, and b is the cell thickness (assumed to be 8 μm). Using the value 25 Ωm obtained by Duncan et al., (1988) we calculate an R_j of approximately 9 MΩ between two cells. Our average value of 15.5 MΩ seems in reasonable agreement. Thus, our isolated cells have many of the same properties of isolated lens epithelial sheets.

Our recording of junctional current between pairs of isolated cells confirms other studies showing electrical communication within the lens epithelium (Schuetze & Goodenough, 1982; Miller & Goodenough, 1986; Duncan et al., 1988; Jacob, 1988; Stewart et al., 1988). The distribution of junctional resistances in our cells was bimodal. One group had a mean corrected resistance of 15.5 MΩ and represented 90% of the cell pairs tested. The other had a mean corrected resistance of 462.9 MΩ and was only 10% of the population. The relationship of this bimodal distribution to the previously reported functionally differentiated junction types

(Schuetze & Goodenough, 1982; Miller & Goodenough, 1986; Duncan et al., 1988) is unclear. On several occasions, we found cells whose initially large coupling resistances decreased with time until they achieved values in the lower resistance population.

The junctional *I-V*s were linear in every one of the 40 cell pairs studied. There was no evidence of voltage-dependent gating. In most preparations studied with the double whole cell technique, the junctional resistances are in the 1–100 MΩ range (Neyton & Trautmann, 1985; Spray et al., 1986; Weingart, 1986; Somogyi & Kolb, 1988). The junctional current in these other preparations is also linear and voltage independent. The junctional *I-V*s had suprisingly little noise. If one assumes identical, independent connexons, the expected standard deviation from the macroscopic current due to channel gating would be

$$\sigma = \{\gamma\mu(V - V_{eq})\,(1 - p_o)\} \qquad (3)$$

where σ is the standard deviation of the macroscopic current, γ is the single-channel conductance (100 pS), V is the transjunctional voltage, V_{eq} is the gap junction channel reversal potential (0 mV), μ is the mean macroscopic current, and p_o is the channel open probability (Colquhoun & Hawkes, 1977). From Figs. 7 and 12, μ = 800 pA, V = 80 mV, γ = 100 pS and assuming p_o = 0.9, then σ = 25 pA. However, since five records were averaged, this number must be divided by $\sqrt{5}$, thus σ = 11 pA. This is in reasonable agreement with the noise estimated from the figure.

We found that the junctions between these cells uncouple spontaneously with a half time of approximately 30 min. A similar time course for uncoupling has been reported by most other investigators using the double whole cell recording technique. Recently, Somogyi and Kolb (1988) found that in pancreatic acinar cells, a combination of 0.1 mM cAMP and 5 mM ATP in the pipette solution increases the half time for uncoupling by a factor of four or more. We found essentially the same result in the frog lens epithelial cells used here.

By recording junctional current well into the period of uncoupling, we were able to observe single gap junction channel openings and closings. This is the first report of such data from intact lens cells. The single-channel conductance in these preliminary recordings was about 100 pS. Given a macroscopic conductance for the junction of about 15 MΩ, this implies at least 650 channels per cell-cell junction. This is a minimum because it assumes unit open probability. To compare these channels with others recorded in mammalian tissues requires that we scale up the conductance to the concentration of mammalian Ringers. The only data we are aware of that addresses the issue of the conductance concentration relation of gap junction molecules comes from the reconstitution experiments on MP26 (Zampighi, Hall & Kreman, 1985). Here the conductance was linear with concentration from 100 mM to 1 M. If this is true for the channels reported here, we would expect a single-channel conductance of around 150 pS in mammalian Ringer. This is comparable to what has been reported in both heart and liver.

Our finding of toxic photodamage by fluorescent dyes must be compared with other reports where significant dye spread was seen in lens and other tissues where damage was not reported (Schuetze & Goodenough, 1982; Cereijido et al., 1984; Safranyos & Caveney, 1985; Zimmerman & Rose, 1985; Spray et al., 1986; Wade, Trosko & Schindler, 1986; Safranyos et al., 1987; Dudek et al., 1988; Duncan et al., 1988). However, many of these studies involved looking at the fluorescent dye spread only after the tissue had been fixed. The dye spread, therefore, occurred in the absence of exciting light. Under these circumstances we also see dye spread. In other studies where the exciting light was on during observation, the dye was injected via conventional microelectrodes. This might allow the cell's natural antioxidants, like glutathione, to handle toxic products. In a whole cell clamp configuration, the cell's contents have largely been replaced by the electrode solution. This exchange may leave the cells with no defense against oxidative damage. However, fluorescent dyes have been placed in cells, with the whole cell clamp technique, without apparent membrane damage (Almers & Neher, 1985). Almers' studies used different dyes than were used here, at lower concentrations and in a different cell type.

It is not unexpected that toxic damage might occur with fluorescent dyes. Such damage has been known for a long time (Miller & Selverston, 1979) and is even the basis of a technique (zap axotomy) to selectively kill cells or parts of cells (Cohan, Hadley & Kater, 1983). In general the damage is thought to be due to the production of O_2 radicals via quenching of the activated flourescent dye. It is well known that the resulting oxygen radicals are toxic. Our demonstration of limited protection with glutathione and ascorbate make it likely that this is the mechanism of damage in this situation.

The whole cell recording technique can be a useful adjunct to studies of whole lens and patch-clamp recording in gathering the data needed to obtain a more complete characterization of lens cell coupling. It also can be useful in gathering the data

on membrane properties necessary to test the lens internal circulation hypothesis (Mathias, 1985). These goals require development of isolated cell preparations from mammalian lens epithelia and from fiber cells. Such preparations are now being developed in many laboratories.

This work was supported by N.I.H. grants EY03282 and EY06005.

References

Almers, W., Neher, E. 1985. The Ca signal from fura-2 loaded mast cells depends strongly on the method of dye-loading. *FEBS Lett.* **192:**13–18

Bettleheim, F.A. 1985. Physical basis of lens transparency. *In:* The Ocular Lens, Structure, Function, and Pathology. pp. 265–300. H. Maisel, editor. Marcel Dekker, New York

Beyer, E.C., Goodenought, D.A., Paul, D.L. 1988. The connexins, a family of related gap junction proteins. *In:* Modern Cell Biology. E.L. Hertzberg and R.G. Johnson, editors. Vol. 7, pp. 167–176. Alan R. Liss, New York

Campos de Carvalho, A.C. 1988. Regulation of gap junctional channels. *Braz. J. Med. Biol. Res.* **21:**177–188

Cereijido, M., Robbins, E., Sabatini, D.D., Stefani, E. 1984. Cell-to-cell communication in monolayers of epithelioid cells (MDCK) as a function of the age of the monolayer. *J. Membrane Biol.* **81:**41–48

Cohan, C.S., Hadley, R.D., Kater, S.B. 1983. 'Zap axotomy': Localized fluorescent excitation of single dye-filled neurons induces growth by selective axotomy. *Brain Res.* **270:**93–101

Colqhoun, C., Hawkes, A.G. 1977. Relaxation and fluctuation of membrane currents that flow through drug operated channels. *Proc. R. Soc. Lond.* **199:**231–262

Cooper, K.E., Tang, J.M., Rae, J.L., Eisenberg, R.S. 1986. A cation channel in frog lens epithelia responsive to pressure and calcium. *J. Membrane Biol.* **93:**259–269

Cota, G., Armstrong, C.M. 1988. Potassium channel "inactivation" induced by soft-glass patch pipettes. *Biophys. J.* **53:**107–109

Dudek, F.E., Gribkoff, V.K., Olson, J.E., Hertzberg, E.L. 1988. Reduction of dye coupling in glial cultures by microinjection of antibodies against the liver gap junction polypeptide. *Brain Res.* **439:**275–280

Duncan, G., Stewart, S., Prescott, A.R., Warn, R.M. 1988. Membrane and junctional properties of the isolated frog lens epithelium. *J. Membrane Biol.* **102:**195–204

Furman, R.E., Tanaka, J.C. 1988. Patch electrode glass composition affects ion channel currents. *Biophys. J.* **53:**287–292

Jack, J.J.B., Noble, D., Tsien, R.W. 1975. Electric Current Flow in Excitable Cells. Clarendon, Oxford

Jacob, T.J.C. 1984. Three types of channel activity in frog lens epithelial cells. *Exp. Eye Res.* **38:**657–660

Jacob, T.J.C. 1988. Fresh and cultured human lens epithelial cells: An electrophysiological study of cell coupling and membrane properties. *Exp. Eye Res.* **47:**489–506

Jacob, T.J.C, Bangham, J.A., Duncan, G. 1985. Characterization of a cation channel on the apical surface of the frog lens epithelium. *Q. J. Exp. Physiol.* **84:**505–534

Marty, A., Neher, E. 1983. Tight-seal whole-cell recording. *In:* Single-Channel Recording. B. Sakmann and E. Neher, editors. pp. 107–122. Plenum, New York

Mathias, R.T. 1985. Steady-state voltages, ion fluxes, and volume regulation in syncytial tissues. *Biophys. J.* **48:**435–448

Mathias, R.T., Rae, J.L. 1989. Cell to cell communication in the lens. *In:* Cell Interactions and Gap Junctions. N. Sperelakis and W.C. Coll, editors. Boca Raton (FL) CRC, *(in press)*

Mathias, R.T., Rae, J.L., Ebihara, L., McMarthy, R.T. 1985. The localization of transport properties in the frog lens. *Biophys. J.* **48:**423–434

Mathias, R.T., Rae, J.L., Eisenberg, R.S. 1979. Electrical properties of structural components of the crystalline lens. *Biophys. J.* **25:**181–201

Miller, J.P., Selverston, A.I. 1979. Rapid killing of single neurons by irradiation of intracellularly injected dye. *Sciences* **206:**702–704

Miller, T.M., Goodenough, D.A. 1986. Evidence for two physiologically distinct gap junctions expressed by the chick lens epithelial cell. *J. Cell Biol.* **102:**194–199

Neyton, J., Trautmann, A. 1985. Single-channel currents of an intercellular junction. *Nature (London)* **317:**331–335

Nicholson, B.J., Takemoto, L.J., Hunkapiller, M.W., Hood, L.E., Revel, J.-P. 1983. Differences between liver gap junction protein and lens MIP26 from rat: Implications for tissue specificity of gap junctions. *Cell* **32:**967–978

Peracchia, C. 1988. The calmodulin hypothesis for gap junction regulation six years later. *In:* Modern Cell Biology. E.L. Hertzberg and R.G Johnson, editors. Vol. 7, pp. 267–284. Alan R. Liss, New York

Rae, J.L. 1984. The patch voltage clamp: Its application to lens research. *Lens Res.* **2:**61–87

Rae, J.L. 1985. The application of patch clamp methods to ocular epithelia. *Curr. Eye Res.* **4:**409–420

Rae, J.L., Germer, H.A. 1974. Junction potentials in the crystalline lens. *J. Appl. Physiol.* **37:**464–467

Rae, J.L., Levis, R.A. 1984. Patch voltage clamp of lens epithelial cells: Theory and practice. *Mol. Physiol.* **6:**115–162

Rae, J.L., Levis, R.A., Eisenberg, R.S. 1988. Ionic channels in ocular epithelia. *In:* Ion Channels. T. Narahashi, editor. Vol. 1, pp. 283–327. Plenum, New York

Revel, J.-P., Yancey, S.B., Nicholson, B., Hoh, J. 1986. Sequence diversity of gap junction proteins. *In:* Junctional Complexes of Epithelial Cells. Ciba Foundation Symposium 125. pp. 108–127. John Wiley & Sons, New York

Rojas, L., Zuazaga, C. 1988. Influence of the patch pipette glass on single acetylcholine channels recorded from *Xenopus* myocytes. *Neurosci. Lett.* **88:**39–44

Safranyos, R.G.A., Caveney, S. 1985. Rates of diffusion of fluorescent molecules via cell-to-cell membrane channels in a developing tissue. *J. Cell Biol.* **100:**736–747

Safranyos, R.G.A., Caveney, S., Miller, J.G., Petersen, N.O. 1987. Relative roles of gap junction channels and cytoplasm in cell-to-cell diffusion of fluorescent tracers. *Proc. Natl. Acad. Sci.* **84:**2272–2276

Schuetze, S.M., Goodenough, D.A. 1982. Dye transfer between cells of the embryonic chick lens becomes less sensitive to CO_2 treatment with development. *J. Cell Biol.* **92:**694–705

Sivac, J.G. 1980. Accommodation in vertebrates: A contemporary survey. *In:* Current Topics in Eye Research. J.A. Zadunaisky and H. Davson, editors. Vol. 3, pp. 281–330. Academic, New York

Somogyi, R., Kolb, H.-A. 1988. Cell-to-cell channel conductance during loss of gap junctional coupling in pairs of pancreatic acinar and Chinese hamster ovary cells. *Pfluegers Arch.* **412:**54–65

Spray, D.C., Ginzberg, R.D., Morales, E.A., Gatmaitan, Z.,

Arias, I.M. 1986. Electrophysiological properties of gap junctions between dissociated pairs of rat hepatocytes. *J. Cell Biol.* **103:**135–144

Spray, D.C., Harris, A.L., Bennett, M.V.L. 1981. Equilibrium properties of a voltage-dependent junctional conductance. *J. Gen. Physiol.* **77:**77–93

Stewart, S., Duncan, G., Marcantonio, J.M., Prescott, A.R. 1988. Membrane and communication properties of tissue cultured human lens epithelial cells. *Invest. Ophthalmol. Vis. Sci.* **29:**1713–1725

Veenstra, R.D., DeHaan, R.L. 1986. Measurement single channel currents from cardiac gap junctions. *Science* **233:**972–974

Wade, M.H., Trosko, J.E., Schindler, M. 1986. A fluorescence photobleaching assay of gap junction-mediated communication between human cells. *Science* **232:**525–528

Weingart, R. 1986. Electrical properties of the nexal membrane studied in rat ventricular cell pairs. *J. Physiol. (London)* **370:**267–284

White, R.L., Spray, D.C., Campos de Carvalho, A.C., Wittenberg, B.A., Bennett, M.V.L. 1985. Some electrical and pharmacological properties of gap junctions between adult ventricular myocytes. *Am. J. Physiol.* **249:**C447–C455

Zampighi, G.A., Hall, J.E., Kreman, M. 1985. Purified lens junctional protein forms channels in planar lipid films. *Proc. Natl. Acad. Sci. USA.* **82:**8468–8472

Zimmerman, A.L., Rose, B. 1985. Permeability properties of cell-to-cell channels: Kinetics of fluorescent tracer diffusion through a cell junction. *J. Membrane Biol.* **84:**269–283

Received 8 November 1988; revised 9 June 1989